NASA TECHNICAL NOTE

NASA TN D-6396

C.1

NASA TN D-6396

TECH LIBRARY KAFB, NM

0132626

LOAN COPY: RETURN TO
AFWL (DOGL)
KIRTLAND AFB, N.

AXIAL AND CIRCUMFERENTIAL VARIATIONS OF HOT-GAS-SIDE HEAT-TRANSFER RATES IN A HYDROGEN-OXYGEN ROCKET

by Ralph L. Schacht and Richard J. Quentmeyer

Lewis Research Center

Cleveland, Ohio 44135

NATIONAL AERONAUTICS AND SPACE ADMINISTRATION • WASHINGTON, D. C. • JULY 1971

TECH LIBRARY KAFB, NM

0132926

1. Report No.	2. Government Accession No.	3. Recipient's Catalog No.
NASA TN D-6396		

4. Title and Subtitle AXIAL AND CIRCUMFERENTIAL VARIATIONS OF HOT-GAS-SIDE HEAT-TRANSFER RATES IN A HYDROGEN-OXYGEN ROCKET	5. Report Date July 1971
	6. Performing Organization Code
7. Author(s) Ralph L. Schacht and Richard J. Quentmeyer	8. Performing Organization Report No. E-5762
	10. Work Unit No. 122-29
9. Performing Organization Name and Address Lewis Research Center National Aeronautics and Space Administration Cleveland, Ohio 44135	11. Contract or Grant No.
	13. Type of Report and Period Covered Technical Note
12. Sponsoring Agency Name and Address National Aeronautics and Space Administration Washington, D.C. 20546	14. Sponsoring Agency Code

15. Supplementary Notes

16. Abstract

An experimental investigation was conducted at the NASA Lewis Research Center to determine the axial and circumferential variations of heat-transfer coefficients in two rocket thrust chambers. Heat-transfer rates were determined from transient temperature measurements at 20 locations in one thrust chamber and at 18 locations in another thrust chamber. The maximum circumferential variation of C in the chamber and throat are 38 and 27 percent, respectively, when Re_d^* was used in the correlating equation $St^* Pr^{*0.7} = C\, Re_d^{*-0.2}$. A satisfactory correlation was obtained for all stations when x was used as the characteristic dimension in Re, with C equal to 0.0215. The standard deviation of C was 0.0038.

17. Key Words (Suggested by Author(s))	18. Distribution Statement
Heat Transfer Engine - Nozzle Design Hydrogen Oxygen Engines	Unclassified - unlimited

19. Security Classif. (of this report)	20. Security Classif. (of this page)	21. No. of Pages	22. Price*
Unclassified	Unclassified	30	$3.00

*For sale by the National Technical Information Service, Springfield, Virginia 22151

AXIAL AND CIRCUMFERENTIAL VARIATIONS OF HOT-GAS-SIDE HEAT-TRANSFER RATES IN A HYDROGEN-OXYGEN ROCKET

by Ralph L. Schacht and Richard J. Quentmeyer

Lewis Research Center

SUMMARY

An experimental investigation was conducted at the NASA Lewis Research Center to determine the axial and circumferential variations of heat-transfer coefficients in two rocket thrust chambers. Heat-transfer rates were determined from transient temperature measurements at 20 locations in one thrust chamber and at 18 locations in another thrust chamber. Heat-flux meters were positioned at six circumferential locations in both the chamber and throat stations. The thrust chambers were operated over a range of mixture ratios from 2.57 to 5.67 (28 to 15 percent hydrogen) at a nominal chamber pressure of 2.068 MN/m^2 (300 psia). Three injectors were used.

Data are correlated on the basis of two equations of the form $St^* \, Pr^{*0.7} = C \, Re_d^{*\,-0.2}$ and $St^* \, Pr^{*0.7} = C \, Re_x^{*\,-0.2}$, where St^*, Pr^*, and Re^* are reference Stanton, Prandtl, and Reynolds numbers, respectively, and C is a constant. The length dimension used to determine the Reynolds number was either the station diameter d or the length from the injector face to the station axial location x. The maximum circumferential variation of C in the chamber and throat are 38 and 27 percent, respectively, when Re_d was used in the correlating equation. The mean values for C for the chamber and throat circumferential surveys were 0.0232 and 0.0184, respectively. This variation was about the same for all three injectors and seemed to be a result of manifold design. A satisfactory correlation was obtained for all stations when X was used as the characteristic dimension in Re, with C equal to 0.0215. The correlation was applicable for pressures of 1.034 and 6.895 MN/m^2 (150 to 1000 psia) and mixture ratios from 2.57 to 8.1 (28 to 11 percent hydrogen). The standard deviation of C was 0.0038.

INTRODUCTION

To effectively design convectively cooled nozzles, a detailed knowledge of the axial and circumferential variation of the hot-gas-side heat-transfer coefficients should be

known. Reference 1 gave some of these details for a hydrogen-oxygen rocket. Since this work was published, numerous inquiries have been received for more detailed information on the axial and circumferential hot-gas-side heat-transfer coefficients, especially in the straight section of the chamber and at the throat. Discoloration patterns on rocket chambers have also caused designers to worry about the effects that the injector and variations in mixture ratio have on the heat-transfer coefficient.

To answer these questions, additional instrumentation was installed and further testing was conducted on two copper heat-sink thrust chambers. These thrust chambers had the same geometry as those of reference 1. Local heat-transfer rates were determined at 20 locations (12 axial stations) for thrust chamber 1 and for 18 locations (five axial stations) for thrust chamber 2. Six circumferential instrumentation sites were incorporated in the chamber and throat axial stations of thrust chamber 2.

Three coaxial injectors were used. One had a copper faceplate and the other two had porous faceplates. One porous faceplate was designed for low chamber pressure (nominal 2.068MN/m^2 or 300 psia) and the other originally for high chamber pressure (nominal 4.147 MN/m^2 or 600 psia). The high-chamber-pressure porous faceplate injector was modified (its fuel elements had been damaged) and then used. This injector was run to determine the effect of misalined and damaged elements on the heat-transfer coefficients.

The thrust chambers were run at a chamber pressure of 2.068 MN/m^2 (300 psia) over a range of mixture ratios from 2.57 to 5.67 (28 to 15 percent hydrogen). The data from reference 1 are also included in this report for correlation purposes.

In the correlation procedure of reference 1, the station diameter was used as the characteristic dimension in the Reynolds number. In this report, the axial distance from the injector face is also used as the characteristic dimension. Comparisons based on these correlations are presented herein for the present rocket data, the rocket data of reference 1, and the heated-air data of reference 2.

INSTRUMENTATION AND DATA RECORDING

Copper rods, 0.635 centimeter (0.25 in.) in diameter and 6.35 centimeters (2.5 in.) long, were used to obtain the transient temperature data. The geometry, construction, installation, sealing, and pressurizing details of these rods are the same as those used in reference 1. Figure 1(a) shows the thermocouple stations on the copper rod. Four chromel-alumel thermocouples were used. Twenty rods at 12 axial stations were used on thrust chamber 1. Eighteen rods at five axial stations were used on thrust chamber 2. Six circumferential locations were incorporated in the chamber (station 2) and throat (station 8) axial stations for thrust chamber 2. A sketch of the chambers along with a table of the instrumentation coordinates is presented in figure 1(a).

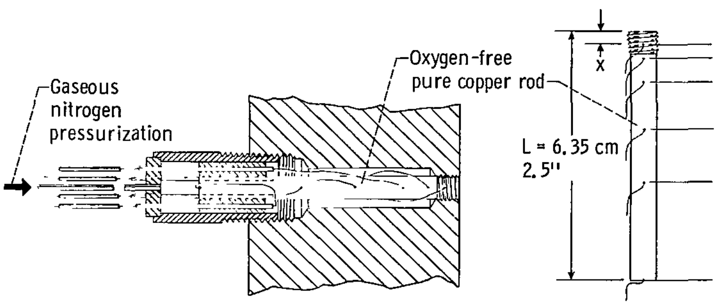

Instrumentation station	Axial distance from throat, x (cm)	Axial distance from throat, x (in.)	Diameter at station, D (cm)	Diameter at station, D (in.)	Area ratio, A/A*	Number of stations, Chamber 1	Number of stations, Chamber 2
1	-29.49	-11.610	27.35	10.77	4.640	2	0
2	-22.21	-8.744	27.35	10.77	4.640	2	6
3	-13.82	-5.440	24.89	9.800	3.842	2	0
4	-5.398	-2.125	16.46	6.67	1.784	2	2
5	-3.597	-1.416	14.90	5.867	1.377	1	0
6	-1.798	-.708	13.22	5.205	1.084	1	0
7 or 8	0	0	12.70	5.00	1.000	2	6
9	1.270	.500	12.96	5.101	1.041	1	0
10	2.540	1.000	13.61	5.359	1.149	1	0
11	3.810	1.500	14.29	5.637	1.267	2	2
12	12.10	4.763	18.74	7.376	2.176	2	0
13	20.39	8.026	23.18	9.125	3.331	2	2

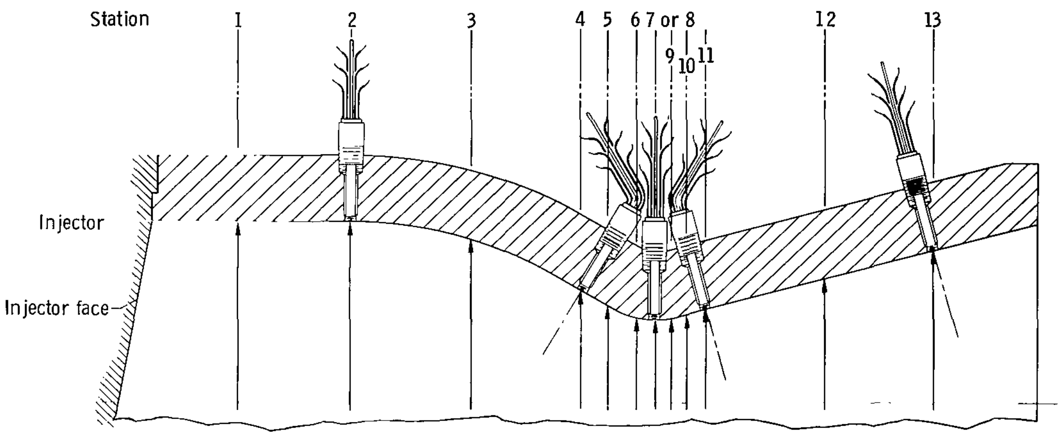

(a) Instrumentation locations and sealing details.

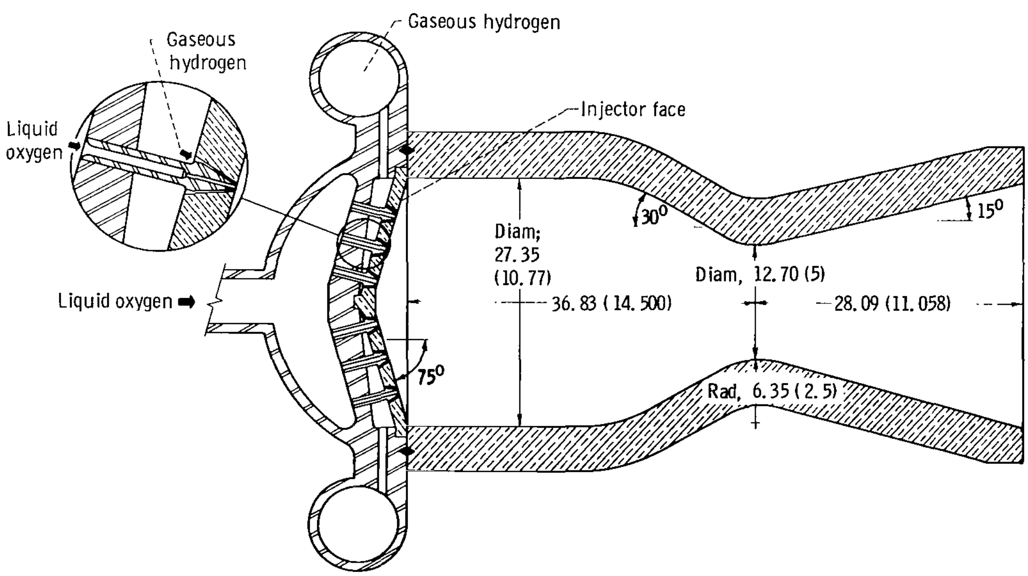

(b) Copper heat-sink rocket thrust chamber with coaxial injector. (All linear dimensions are in centimeters (in.).)

Figure 1. - Instrumentation.

Static pressure measurements were taken at all stations except at the 29.49- and 22.21-centimeter (11.61- and 8.744-in.) axial locations for thrust chamber 2. The measured chamber pressure was used as the static pressure for these two stations, which are in the constant diameter position of the chamber. The theoretical static pressure was used at all stations for thrust chamber 2.

A venturi and orifice were used to measure the oxygen and hydrogen flows, respectively. Temperatures and pressures were recorded on a digital recording system that had a sampling rate of 31 250 words per second with a block length of 125 words. Data parameters were fitted over a 25-word sampling interval with smoothing to eliminate 60-hertz noise and greatly diminish any random noise. A smooth curve was fit through 25 readings of the data parameter, and then one reading, to be used in the terminal calculations, was made for all parameters at a common time. This reduced the amount of terminal calculations. Chamber pressure, which was sampled many times in each data block, was used as a triggering device for starting and stopping the calculations. These data were used to evaluate the performance as well as the heat transfer. The heat-transfer coefficients that were calculated from three thermocouples on each rod were averaged. The average was used in the correlation procedures.

APPARATUS AND EXPERIMENTAL PROCEDURE

In this investigation, two copper heat-sink, solid-wall thrust chambers were used to obtain transient temperature data. Figure 1(b) gives the geometry of the thrust chambers.

Three coaxial injectors were used with liquid oxygen and gaseous hydrogen as the propellants. Each of the injectors had 234 injector elements uniformly spaced in a circular pattern (0.4 element/cm^2 or 2.6 elements/in.^{2}). The injector faceplates were dish shaped. One faceplate (injector 1) was made of solid copper and the other two were made of porous Rigimesh stainless steel material. The Rigimesh was used to give the faceplate transpiration cooling (fig. 2). Injector 1 had oxygen tubes that had fins to center the oxygen element. No fins were used on the oxygen tubes that were used with Rigimesh faceplates. One porous faceplate injector (injector 2) was designed for low chamber pressure (nominal 2.06 MN/m^2 or 300 psia) and the other (injector 3) was designed for high chamber pressure (nominal 4.137 MN/m^2 or 600 psia). Originally, the oxygen and hydrogen hole sizes were the only difference between the two designs. The holes were sized for a 689-kN/m^2 (100-psi) pressure drop at chamber pressures of 2.068 MN/m^2 (300 psia) and 4.137 MN/m^2 (600 psia). Injector 3, which originally was the high chamber pressure design, was used in this heat-transfer study to find the effects of misalinement and concentricity of elements on the heat-transfer coefficients. The misalinement

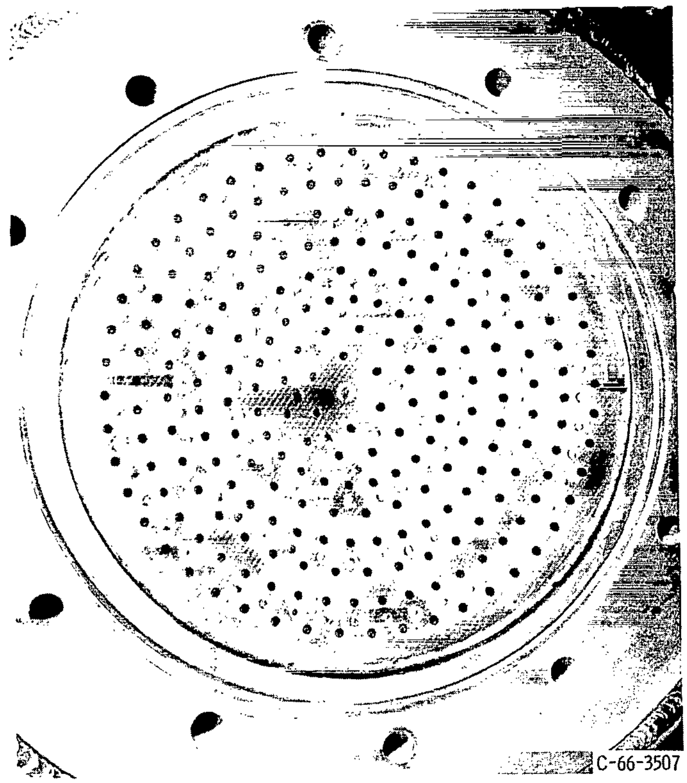

Figure 2. - Injector porous faceplate.

was caused by damage from many previous runs. The oxygen holes in this injector were bushed down to the same size as the low-chamber-pressure Rigimesh design so only the hydrogen feed holes were larger than injectors 1 and 2. Injector 3, which was a high-chamber-pressure design, was modified to run at low chamber pressures. Thus, the results from the injectors could be compared under similar operating conditions.

The test runs were made on a test stand located at the Lewis Plum Brook Facility. Figure 3 shows the copper heat-sink thrust chamber installed in the test facility. Propellent valves for controlling gaseous hydrogen and liquid oxygen were positioned before the run and opened to these fixed positions during the run to provide a step rise in chamber pressure. Once the nominal chamber pressure had been achieved, an automatic control took over and repositioned the valves to give exact values of chamber pressure and mixture ratios so that runs with different injectors could be repeated with identical flow conditions. All runs were made at a chamber pressure of 2.068 MN/m^2 (300 psia) with mixture ratios varied from 2.57 to 5.67 (28 to 15 percent hydrogen). Full chamber pressure was achieved in 0.02 to 0.06 second. This step function in chamber pressure or driving temperature made it possible to use a simpler mathematical model to obtain heat-transfer coefficients.

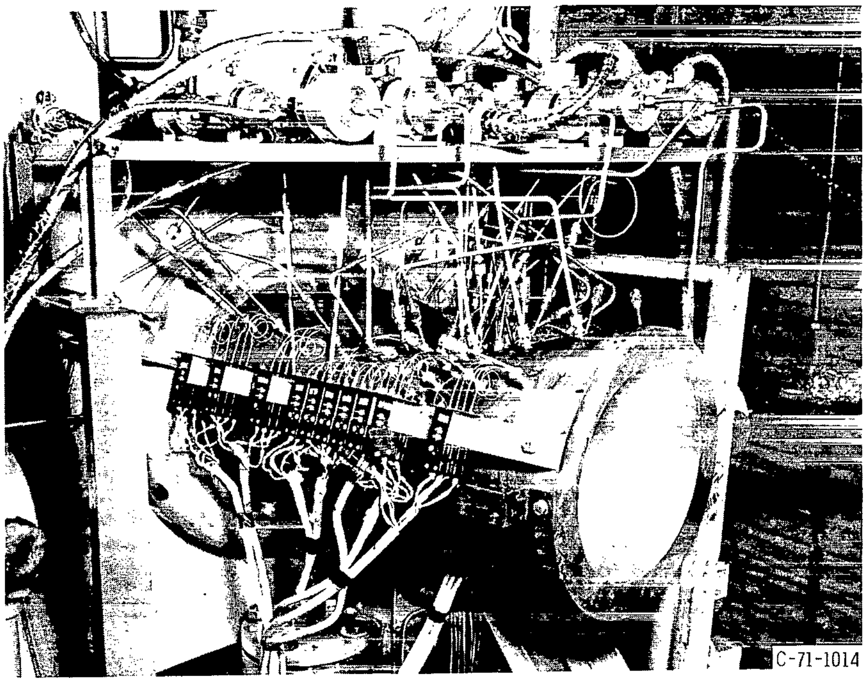

Figure 3. - Copper heat-sink rocket thrust chamber on test stand.

CALCULATION PROCEDURE

The calculation procedure used to find the heat-transfer coefficient was the constant h method as used in reference 1. (Symbols are given in the appendix.)

The equation used for the solution of h from the one-dimensional semi-infinite slab as given in reference 3 is

$$\frac{T - T_0}{T_{AW} - T_0} = \text{erfc}\,\frac{\frac{hx}{k}}{2\sqrt{\frac{h^2t}{k\rho c}}} - e^{\left[(hx/k) + (h^2t/k\rho c)\right]}\,\text{erfc}\left(\frac{\frac{hx}{k}}{2\sqrt{\frac{h^2t}{k\rho c}}} + \sqrt{\frac{h^2t}{k\rho c}}\right)$$

where

$$\text{erfc}\,(Z) = 1 - \frac{2}{\pi}\int_0^{(Z)} e^{-Z^2}\,dZ$$

This equation was programmed so that an iteration process found the h that satisfied the measured T for a given location x on the rod and time t. The initial condition

is $T = T_0$ at $t = 0$. The material properties (k, ρ, c) were evaluated at a temperature $(T_{x=0} - T_0)/4 + T_0$ (ref. 1).

The nondimensional heat-transfer parameters were computed by introducing the transport properties as a function of reference enthalpy H^* (ref. 4) and static pressure P_s where $H^* = H_s + 0.5 (H_w - H_s) + 0.22 (Pr^*)^{1/3} (H_c - H_s)$. Numerous programs are presently in existence for the calculation of equilibrium compositions and other thermodynamic properties of complex chemical systems. The programs of reference 5 for thermodynamic properties and of reference 6 for transport properties were modified and simplified for a gaseous-hydrogen - liquid-oxygen system by Frederic N. Goldberg of Lewis.

Before the heat-transfer coefficient h can be computed, the driving temperature T_{AW} must be determined throughout the nozzle; to determine T_{AW}, the combustion temperature must be known. Combustion temperature is a function of combustion chamber pressure, percent fuel, and combustion efficiency. The program was further modified to account for combustion efficiency and is described in reference 1.

Two conditions were spelled out in reference 1: When the combustion efficiency was less than 1, an iteration was performed whereby combustion temperature was reduced until the measured weight flow and chamber pressure produced $M = 1$ at the throat; when the combustion efficiency was greater than 1, the theoretical combustion temperature was used and the weight flow was adjusted to produce $M = 1$ at the throat.

The average combustion efficiency obtained from all the test data was 98 percent of theoretical equilibrium. A 2-percent change in combustion efficiency results in a change of heat-transfer coefficient of about 2 percent.

For thrust chamber 1, T_{AW} was determined for each station in the convergence, throat, and divergence sections by using the measured static pressure ratio instead of area ratio.

RESULTS AND DISCUSSION

Axial Variation of Correlation Constant C

A correlation of the form $St^* \, Pr^{*0.7} = C \, Re_d^{*-0.2}$ was used in reference 1, where St^*, Pr^*, and Re_d^* are reference Stanton, Prandtl, and Reynolds numbers, respectively, and C is a constant for any one axial station. Figure 4(a) shows the variation in C with axial distance for 12 axial locations in thrust chamber 1 for various mixture ratios.

The C variation with axial distance results for reference 1 and the mean values for the various mixture ratios for the present results are shown on figure 4(b). The values

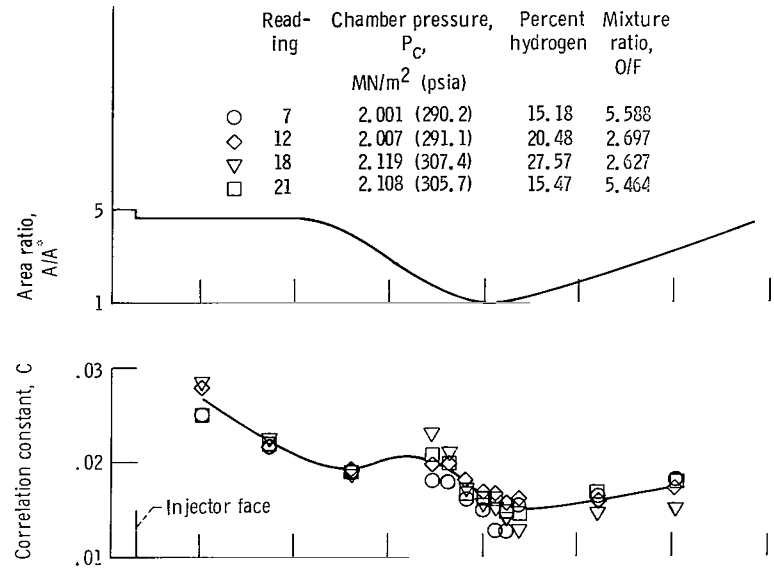

(a) Correlation constant as function of axial distance for various mixture ratios.

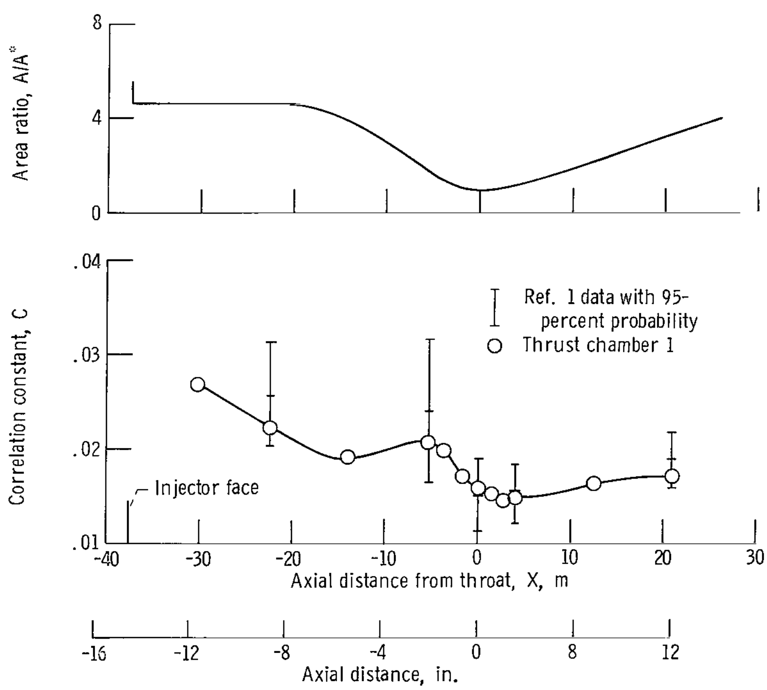

(b) Correlation constant comparison of present data to that of reference 1.

Figure 4. - Correlation constants.

of C for reference 1 are the mean values for chamber pressures from 1.03 to 6.845 MN/m^2 (150 to 1000 psia) and for mixture ratios from 4.88 to 8.10 (17 to 11 percent hydrogen). To show the spread of C, the 95-percent probability of the data from reference 1 is also shown for these data. The data from the present tests are in good agreement with the results from reference 1 and show additional detail because more axial instrumentation locations were used. The C values extrapolated to the injector face indicate higher values than would be inferred from reference 1.

At any one station, this equation does a good job of correlating the results over a range of fuel percentages using the mean value of C. In other words, the use of reference enthalpy and static pressure for getting the transport properties in the correlating equation adequately accounts for variable properties.

Circumferential Variation of the Correlation Constant C

Table I shows the variation of h, C, T_{AW}, and T_0 with circumferential location. Since the data were all taken by a transient technique, the reported values are not all for the same time for each injector; therefore, the absolute values of the wall temperature should not be used in comparing the results for the various injectors. The heat-transfer coefficient h or the correlating constants C can be compared.

Figure 5(a) shows a plot of C as a function of circumferential location for the chamber (axial position, -22.21 cm or -8.744 in.) and the injectors used with thrust chamber 2. The C was obtained from the correlation $St^* \, Pr^{*0.7} \, Re_d^{*0.2} = C$. Figure 5(b) shows a plot of the same variables for the throat position. Figure 5 shows that the data for all the injectors have about the same trends in amplitude and shape. The damaged element injector (modified high P_c, porous, injector 3) gives the same variation in the constant C as the other injectors. The circumferential variations in h or C for the worst cases were 38 percent in the chamber and 27 percent at the throat. Regardless of how the thrust chamber was positioned with respect to the injector, a temperature sensing plug was always alined with an injector element. This was true even for the results of the modified high-chamber-pressure porous injector (3) where the nozzle was rotated 30° with respect to the injector. Therefore, the amplitude shown in figure 5(a) cannot be attributed to the misalinement of sensing plug and injector elements.

Figure 5(a) shows an arrow indicating the gaseous hydrogen manifold inlet angular position. There is only one hydrogen inlet. This position coincides with the lowest C's for all injectors. Another region of low C's, 180° from this position, suggests that the manifolding might cause two hydrogen rich regions and two hydrogen starved regions in the chamber.

TABLE I. - PERFORMANCE AND HEAT TRANSFER

Reading	Chamber pressure, P_c: MN/m²	Chamber pressure, P_c: psia	Percent fuel	Mixture ratio, O/F	Combustion efficiency	Type of injector	Time, sec	Area	Circumferential location: deg	Circumferential location: radians	Heat-transfer coefficient, h: kW/(m²)(K)	Heat-transfer coefficient, h: Btu/(ft²)(sec)(°R)	Constant, C	Adiabatic wall temperature, T_{AW}: K	Adiabatic wall temperature, T_{AW}: °R	Wall temperature, T_w: K	Wall temperature, T_w: °R	Initial temperature, T_0: K	Initial temperature, T_0: °R	Heat flow rate per unit area, q: MW/m²	Heat flow rate per unit area, q: Btu/(ft²)(sec)
24	2.083	302.1	15.64	5.934	1.00	Low P_c, porous	1.732	Chamber	105	1.833	2.537	0.1242	0.02459	3340.1	6012.2	567.9	1022.3	273.1	491.5	7.032	619.6
									165	2.880	2.128	.1042	.02069			526.1	946.9	278.5	501.3	5.992	528.0
									225	3.927	2.024	.0991	.01968			510.7	919.3	274.3	493.8	5.726	504.5
									285	4.974	2.935	.1437	.02838			613.2	1103.8	280.2	504.4	8.008	705.6
									345	6.021	2.284	.1118	.02218			538.8	968.0	273.0	491.4	6.401	564.0
									45	.7854	2.178	.1066	.02116			526.7	948.0	273.4	492.1	6.127	539.9
								Throat	105	1.833	6.406	0.3136	0.01589	3263.0	5873.5	924.5	1664.1	284.6	512.2	14.980	1320.0
									345	6.021	7.237	.3543	.01782			990.4	1782.8	283.6	510.5	16.446	1449.1
									225	3.927	6.426	.3146	.01594			925.4	1665.7	283.6	510.4	15.021	1323.6
									285	4.974	7.072	.3462	.01744			976.4	1757.6	282.2	508.0	16.171	1424.9
									165	2.880	7.301	.3574	.01797			991.6	1784.9	278.5	501.3	16.583	1461.2
									45	.7854	8.461	.4142	.02058			1082.5	1948.5	282.7	508.8	18.449	1625.6
27	2.092	303.4	15.38	5.502	1.00	High P_c, porous	1.916	Chamber	105	1.833	2.962	0.1450	0.02856	3355.2	6039.5	640.9	1153.7	288.7	519.7	8.040	708.4
									165	2.880	2.431	.1190	.02354			582.6	1048.7	288.7	519.7	6.740	593.9
									225	3.927	2.341	.1146	.02268			572.2	1029.9	288.3	518.9	6.514	574.0
									285	4.974	2.807	.1374	.02710			627.0	1128.6	291.9	525.4	7.659	674.9
									345	6.021	2.482	.1215	.02402			587.1	1056.8	287.3	517.2	6.871	605.4
									45	.7854	2.206	.1080	.02140			556.5	1001.8	287.7	517.9	6.175	544.1
								Throat	105	1.833	8.026	0.3929	0.01942	3277.2	5899.0	1088.7	1959.6	287.7	517.9	17.565	1547.7
									345	6.021	7.570	.3706	.01842			1053.2	1895.8	288.1	518.6	16.837	1483.6
									225	3.927	8.692	.4255	.02088			1138.9	2050.0	287.6	517.7	18.587	1637.8
									285	4.974	8.077	.3954	.01955			1093.3	1967.9	288.1	518.6	17.650	1555.2
									165	2.880	7.785	.3811	.01889			1070.7	1927.3	288.7	519.7	17.180	1513.8
									45	.7854	8.967	.4390	.02146			1164.1	2095.4	294.0	529.2	18.952	1669.9

30	2.070	300.2	15.42	5.485	0.9982	High P_c,	1.876	Chamber	75	1.309	2.578	0.1262	0.02531	3396.3	6011.4	583.5	1050.4	276.5	497.7	7.108	626.3
						porous			135	2.356	2.298	.1125	.02260			550.8	991.5	274.7	494.4	6.410	564.8
						rotated			195	3.403	2.400	.1175	.02360			559.3	1006.7	271.3	488.4	6.675	588.2
						30^{o}			255	4.450	2.788	.1365	.02733			604.9	1088.8	274.9	494.9	7.625	671.9
						counter-			315	5.498	2.641	.1293	.02592			586.0	1054.8	271.6	488.8	7.275	641.0
						clockwise			15	.2618	2.343	.1147	.02303			552.1	993.8	270.6	487.1	6.529	575.3
								Throat	75	1.309	7.533	0.3688	0.01868	3262.5	5872.5	1034.6	1862.3	280.6	505.1	16.785	1479.0
									315	5.498	8.357	.4091	.02055			1096.7	1974.0	278.7	501.6	18.099	1594.8
									195	3.403	8.500	.4161	.02087			1107.8	1994.1	279.9	503.9	18.316	1613.9
									255	4.450	8.130	.3980	.02004			1080.4	1944.8	279.8	503.7	17.742	1563.3
									135	2.356	8.506	.4164	.02089			1104.9	1988.9	274.7	494.4	18.353	1617.2
									15	.2618	10.11	.4951	.02442			1215.9	2188.6	268.9	484.0	20.698	1823.8
31	2.095	303.9	15.60	5.410	0.9885	Low P_c,	1.772	Chamber	105	1.833	2.696	0.1320	0.02652	3266.5	5879.8	591.5	1064.8	288.6	519.4	7.213	635.6
						copper			165	2.880	2.037	.09978	.02009			523.9	943.1	290.4	522.8	5.590	492.6
						face-			225	3.927	2.094	.10250	.02063			528.2	950.7	288.7	519.6	5.732	505.1
						plate			285	4.974	2.635	.1290	.02593			586.1	1055.0	289.7	521.4	7.064	622.4
									345	6.021	2.079	.1018	.02048			525.2	945.3	287.1	516.7	5.698	502.1
									45	.7854	2.196	.1075	.02164			537.8	968.1	287.2	516.7	5.993	528.1
								Throat	105	1.833	7.364	0.3605	0.01865	3195.1	5751.2	997.2	1794.9	292.4	526.4	16.184	1426.0
									345	6.021	6.104	.2988	.01588			896.4	1613.6	291.1	524.0	14.056	1238.5
									225	3.927	7.315	.3581	.01853			994.2	1789.5	293.6	528.5	16.098	1418.5
									285	4.974	6.357	.3112	.01620			916.4	1649.5	290.3	522.5	14.487	1276.5
									165	2.880	5.903	.2890	.01508			884.0	1591.3	296.4	533.5	13.643	1202.1
									45	.7854	6.896	.3376	.01752			959.0	1726.2	290.0	522.0	15.420	1358.7
37	2.098	304.3	20.39	3.904	0.9962	Low P_c,	2.040	Chamber	105	1.833	3.062	0.1499	0.02728	2978.6	5361.5	622.4	1120.3	295.7	532.2	7.216	635.8
						copper			165	2.880	2.178	.1066	.01931			534.3	961.8	295.3	531.5	5.320	468.8
						face-			225	3.927	2.167	.1061	.01922			532.6	958.6	294.4	529.9	5.301	467.1
						plate			285	4.974	2.698	.1321	.02490			586.5	1055.8	295.3	531.5	6.454	568.7
									345	6.021	2.130	.1043	.01889			527.4	949.3	292.9	527.2	5.222	460.1
									45	.7854	2.265	.1109	.02011			541.2	974.2	292.8	527.0	5.525	486.8
								Throat	105	1.833	7.239	0.3544	0.01729	2921.5	5258.7	961.7	1731.0	297.1	534.8	14.185	1249.9
									345	6.021	6.428	.3147	.01533			900.2	1620.4	295.4	531.8	12.993	1144.9
									225	3.927	7.237	.3543	.01729			960.9	1729.6	296.4	533.5	14.190	1250.3
									285	4.974	6.812	.3335	.01626			928.0	1670.5	294.0	529.2	13.579	1196.5
									165	2.880	6.637	.3249	.01583			916.0	1648.8	295.3	531.5	13.310	1172.8
									45	.7854	7.699	.3769	.01840			993.2	1787.8	295.3	531.5	14.845	1308.1

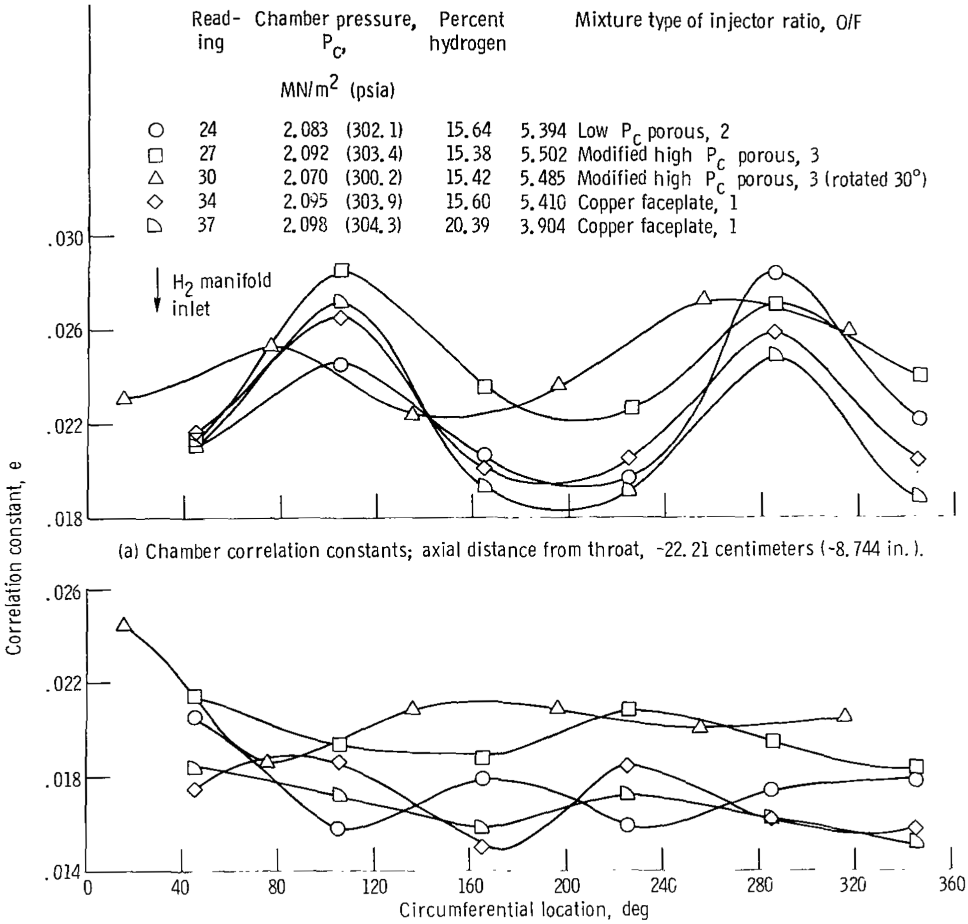

(a) Chamber correlation constants; axial distance from throat, -22.21 centimeters (-8.744 in.).

(b) Throat correlation constants; axial distance from throat, 0.

Figure 5. - Correlation constants for various injectors.

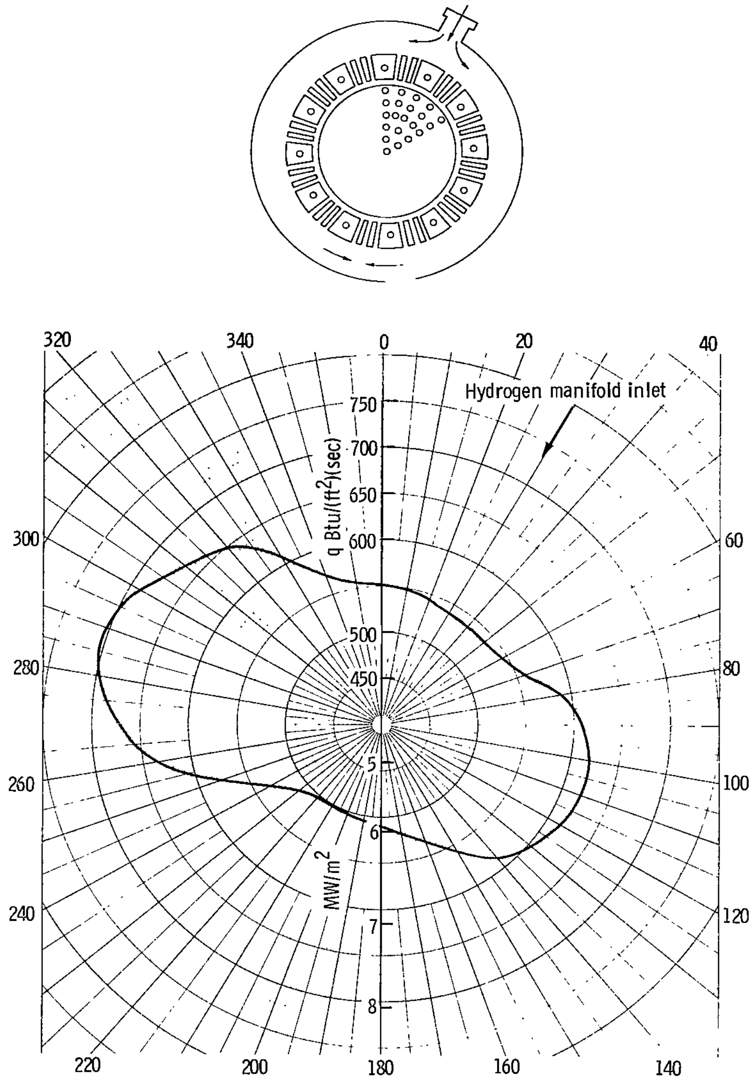

Figure 6. - Chamber heat input q as function of angular position for reading 24.

Figure 6 shows a sketch of the injector showing the angular location of the hydrogen manifold inlet. The circumferential variation of heat input q, as determined from the instrumented rods, is also shown on this figure for reading 24. Again, these variations are shown to be lowest at locations in line with and opposite to the inlet line of the hydrogen manifold.

Analysis of the Effect of Input Specifications on Calculations of the Heat-Transfer Coefficient

The C's and q's presented in figures 5 and 6 were computed with driving temperatures that corresponded to the chamber pressures and percent fuels measured at the injector and listed in table I. Hereafter, this will be called input specification 1.

To study this variation in more detail, two more input specifications will be studied using reading 24. These variations will only be studied at two angular positions corresponding to the regions of highest and lowest q's.

Reading 24, for example, could be recomputed where the driving temperature T_{AW} could be considered a function of the zone, that is, by allowing the percent fuel to vary. The highest wall temperature T_W (613.2 K or 1103.8° R) will give a heat-transfer coefficient h of 2.801 kW/(m^2)(K) (0.1371 Btu/(ft^2)(sec)(°R)). Assuming h constant circumferentially, this h with the lowest wall temperature measured (510.7 K or 919.3° R) requires a driving temperature of 2541 K (4575° R). This temperature corresponds to 24 percent hydrogen. The h used here is the lowest h that can be used for both the highest and lowest wall temperatures measured. Any lower h would require a T_{AW} greater than stoichiometric to get the highest wall temperature. Hereafter, this type of calculation will be called input specification 2.

Another way to handle the data would be to assume that a flat plate correlation of the form $St^* \, Pr^{*0.7} = 0.0295 \, Re_x^{*-0.2}$ (hereafter called input specification 3) and that the correlating constant (0.0295) should be applicable at all circumferential positions at the station x = -22.21 centimeters (-8.744 in.). Then the measured values of q and T_W could be used to determine the range of T_{AW} that would be necessary to satisfy these conditions.

For reading 24 (table I) at an angular position of 285°, use of a T_{AW} of 3340° K (6012° R) resulted in an h of 2.935 kW/(m^2)(K) (0.1437 Btu/(ft^2)(sec)(°R)) and a correlation

$$St^* \, Pr^{*0.7} = 0.02838 \, Re_d^{*-0.2}$$

Using a flat-plate correlation with axial length instead of diameter as the characteristic dimension results in

$$\mathrm{St}^* \ \mathrm{Pr}^{*0.7} = 0.02504 \ \mathrm{Re}_x^{*\,-0.2}$$

The heat-transfer coefficient h is relatively insensitive to changes in percent fuel. Therefore, the ratio of h's can be formed

$$\frac{h}{0.1437} = \frac{0.0295}{0.02504}$$

to yield $h = 0.1693$, which is consistent with a flat-plate correlation with a constant of 0.0295. To satisfy a q of 8.008 MN/m^2 (705.6 Btu/(ft^2)(sec)) and a wall temperature of 613.2 K (1103.8° R), T_{AW} would have to be 2928 K (5271° R). With an h of 3.458 kW/(m^2)(K) (0.1693 Btu/(ft^2)(sec)($^\circ$R)), a T_W of 510.7 K (919.3° R), and a q of 5.726 MW/(m^2)(sec) (504.5 Btu/(ft^2)(sec)), T_{AW} would have to be 2166 K (3899° R). These temperatures correspond to a mixture ratio of 4 and 2.45 (20 and 29 percent hydrogen). The mixture ratio supplied to the injector was 5.934 (15.64 percent hydrogen).

The following table summarizes the three input specifications for calculating the circumferential variations observed at station 2 in the chamber for reading 24. The calculations illustrate that what is really measured in the rods is the heat flow rate q, and one has the problem of separating h and T_{AW}. Input specification 1 assumes a constant T_{AW} at all circumferential locations. The T_{AW} is that computed from the measured

Input specification	Heat flow rate and wall temperature values	Heat-transfer coefficient, h		Adiabatic wall temperature, T_{AW}		Percent fuel
		$\frac{kW}{(m^2)(K)}$	$\frac{Btu}{(ft^2)(sec)(^\circ R)}$	K	$^\circ$R	
1. Constant T_{AW}, constant percent fuel	Highest	2.935	0.1437	3340	6012	15.64
	Lowest	2.024	.0991	3340	6012	15.64
2. Constant h circumferentially, highest percent fuel = stoichiometric	Highest	2.801	0.1371	3340	6012	11.2
	Lowest	2.801	.1371	2540	4575	24
3. Constant C circumferentially, $\mathrm{St}^* \ \mathrm{Pr}^{*0.7} = 0.0295 \ \mathrm{Re}_x^{*\,-0.2}$	Highest	3.458	0.1693	2928	5271	20
	Lowest	3.458	.1693	2166	3899	29

P_c and percent fuel supplied to the injector. Specification 2 assumes a constant h at all circumferential locations and gives a variation of T_{AW} that goes along with a variation from stoichiometric (11.2 percent) to 24 percent hydrogen. Specification 3 assumes a constant C at all circumferential locations that goes along with a heat-transfer correlation of the form

$$St^* \, Pr^{*0.7} = 0.0295 \, Re_x^{*-0.2}$$

This results in a variation of T_{AW} that goes along with a variation of mixture ratio of 4 to 2.45 (20 to 29 percent hydrogen.) The measured mixture ratio at the injector was 5.934 (15.64 percent hydrogen).

The preceding calculations, although they do not pinpoint h exactly, do indicate rough limits that warn a designer that a good injection process and good manifolding must be used in order to avoid circumferential variations in heat transfer. Figure 5(b) shows that by the time the throat is reached, the pattern of C varying with angular position is no longer observed. These are the only two axial locations where detailed heat-transfer circumferential data were taken, and all figures showing axial heat-transfer detail indicate averages of the measurements at any one axial location. Since T_{AW} was not measured, the driving temperatures used in the results for the rest of the report are those that go with the measured chamber pressure and percent fuel supplied to the injector (specification 1).

To see how the circumferential variation would affect the wall temperatures in a liquid cooled thrust chamber design, a 15-percent variation in the hot-gas-side heat-tranfer coefficient was made. The thrust chamber used to analytically evaluate these wall temperature changes was a liquid-hydrogen cooled research chamber that had 347 stainless-steel coolant tubes with 25-millimeter (0.010 in.) wall thicknesses. The coolant tubes were designed to simulate a nuclear rocket; that is, all propellant went through the coolant passages. The inlet conditions were 4.82-MN/m^2 (700-psia) coolant pressure at a bulk temperature of 27.8 K (50^o R). At a chamber pressure of 2.068 MN/m^2 (300 psia), this 15-percent variation caused the throat wall temperature to change by approximately 111.1 K (200^o R). The chamber and exit wall temperature changed approximately 55.56 K (100^o R). These magnitudes of wall temperature variation could be important in a critical design.

Correlation Using Reynolds Number Based on Axial Distance

The previous correlations in which Re was based on the local diameter do a reasonable job of predicting h, provided that the local value of C is known (for a given station, the property evaluation at reference enthalpy handles various mixture ratios and chamber pressures). However, in a new engine geometry, the designer must determine the proper

axial distribution of the constant C. Van Glahn in reference 7, because of the complexity of nozzle heat transfer, gives several correlating equations in order to accommodate the several heat-transfer regimes as defined by Reynolds number and geometric locations.

In attempting to find a simpler correlation that could universally be used, $St^* \, Pr^{*0.7}$ data were plotted as a function of Reynolds number based on axial length from the injector face. In determining this correlation, the geometry of a high-contraction-ratio, large nozzle was assumed to more closely approximate a flat plate than a tube. Figure 7 shows plots of these data and also the data of reference 1 for the various axial stations. Figure 7(c), which is the throat station, indicates that a slope other than -0.2 would better fit the data; however, the range of Reynolds number covered by the data is small. The middle ▽ symbols on this curve and that of figure 6 are the mean values of C for four runs at a chamber pressure of 2.068 MN/m^2 (300 psia) and a mixture ratio of 5.67 (15 percent hydrogen) for six circumferential stations. The upper and lower ▽ symbols are the average of the highest and lowest C's for these four runs. These limits are repeated here to show the circumferential variation on a Re_x basis.

Figure 8 is a plot of the correlation constant C as a function of axial distance along the nozzle. The solid line connects C's computed from the equation

$$C = St^* \, Pr^{*0.7} \, Re_x^{*0.2}$$

and the dashed line connects C's computed from the equation

$$C = St^* \, Pr^{*0.7} \, Re_d^{*0.2}$$

When using x for the characteristic dimension in the Reynolds number, the variation in C is reduced by a factor of two. Figure 8 also indicates that the heat-transfer correlating constant C in the throat region is not much different from the average for the whole thrust chamber when put on a Re_x basis. In other words, acceleration or other effects in the throat region for this thrust chamber do reduce the C used in predicting the heat-transfer coefficient, but only about 10 percent below the average C for the whole thrust chamber. Acceleration or other effects in the throat region of a nozzle when based on an Re using diameter as the characteristic dimension normally reduce C at the throat by approximately 40 percent below that value of C in the chamber (ref. 1).

Figure 9(a) shows a plot of $St^* \, Pr^{*0.7}$ as a function of Re_x^* for a chamber pressure of 2.117 MN/m^2 (307 psia) and mixture ratio of 2.64 (27.5 percent hydrogen) for all axial stations. Figure 9(b) is a plot of the same data as a function of Reynolds number based on the diameter. Figure 9 shows a typical correlating line for heating in tubes where 0.026 is used as the constant. One sees that using x for the characteristic dimension

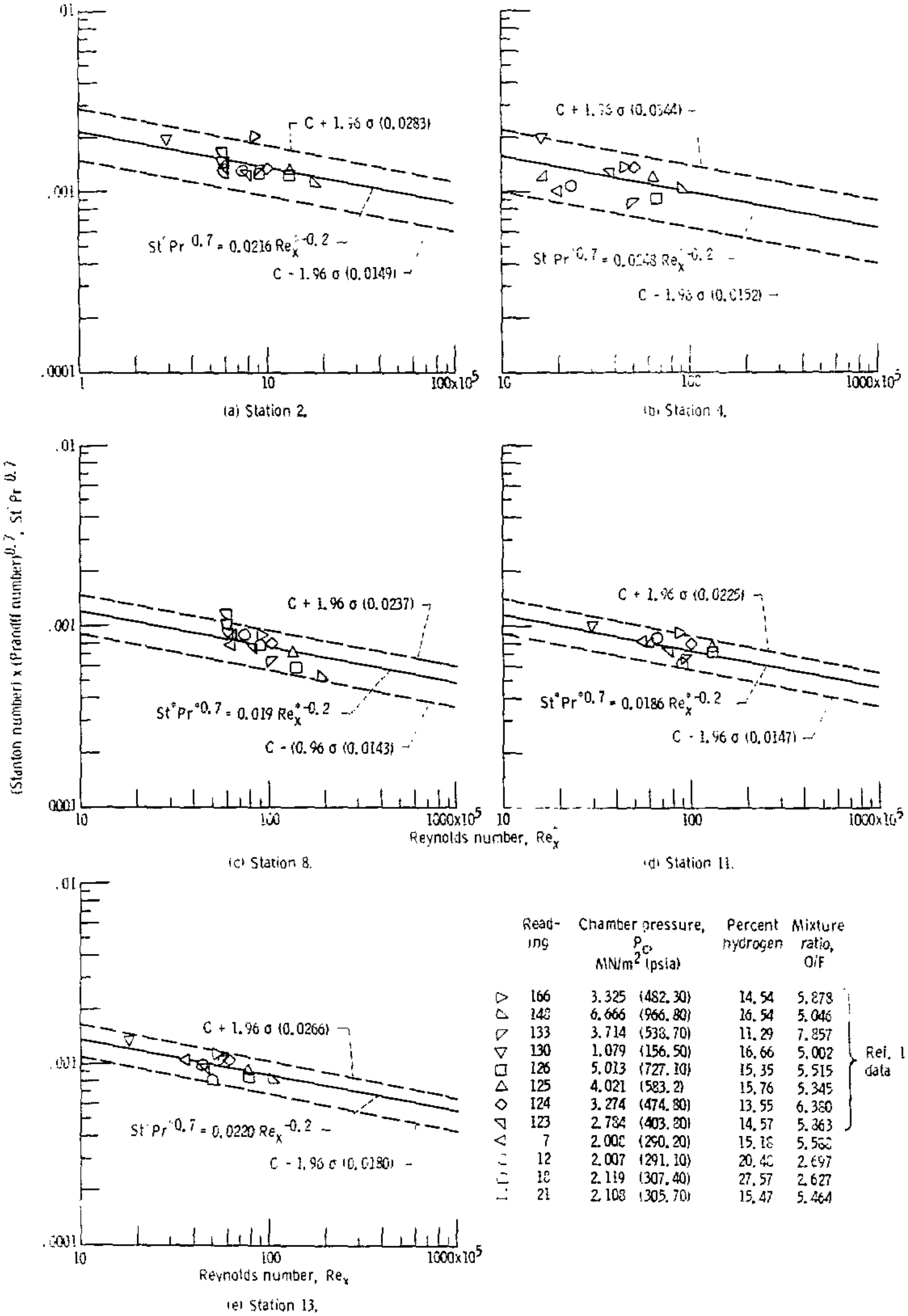

	Reading	Chamber pressure, P_c, MN/m^2 (psia)	Percent hydrogen	Mixture ratio, O/F
▷	166	3.325 (482.30)	14.54	5.878
◺	148	6.666 (966.80)	16.54	5.046
◸	133	3.714 (538.70)	11.29	7.857
▽	130	1.079 (156.50)	16.66	5.002
□	126	5.013 (727.10)	15.35	5.515
△	125	4.021 (583.2)	15.76	5.345
◇	124	3.274 (474.80)	13.55	6.380
◁	123	2.784 (403.80)	14.57	5.363
◁	7	2.008 (290.20)	15.18	5.568
◠	12	2.007 (291.10)	20.40	2.697
⌂	18	2.119 (307.40)	27.57	2.627
⌒	21	2.108 (305.70)	15.47	5.464

Figure 7. - Product of station number and Prandtl numbers as function of Reynolds number

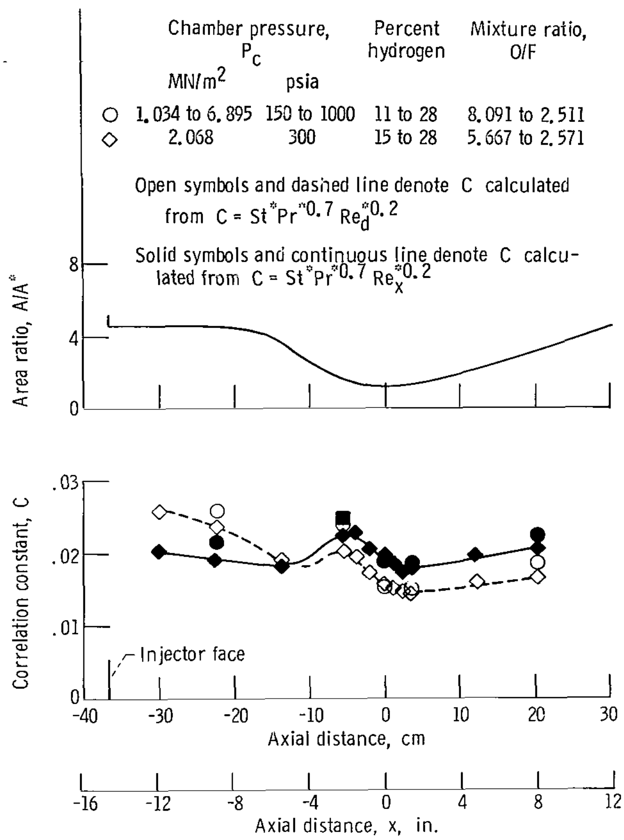

Figure 8. - Comparison of correlation constants calculated using Reynolds number based on station diameter and using Reynolds number based on distance from injector force.

	Station	Axial distance, x, cm	(in.)	Area ratio, A/A^*
○	1	-29.49	(-11.610)	4.64
□	2	-22.21	(-8.744)	4.63
◇	3	-13.82	(-5.440)	3.84
△	4	-5.398	(-2.125)	1.78
◺	5	-3.597	(-1.416)	1.38
D	6	-1.798	(-.708)	1.08
◊	7	0	(0)	1.00
◇	9	1.27	(.500)	1.04
⌂	10	2.54	(1.000)	1.15
▽	11	3.81	(1.500)	1.27
◸	12	12.10	(4.763)	2.18
◡	13	20.39	(8.026)	3.33
◹	Refer to figs. 7(a) and 7(c)			

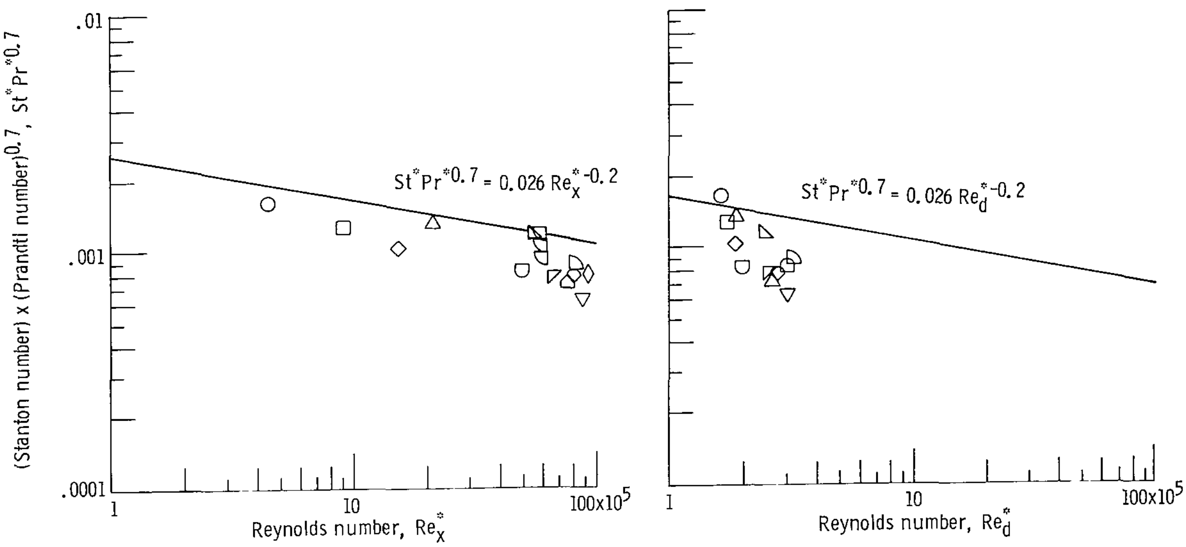

(a) Reynolds number based on axial distance from injector face.

(b) Reynolds number based on diameter.

Figure 9. - Product of Stanton number and (Prandtl number)$^{0.7}$ as function of Reynolds number for various axial positions. Reading 18; chamber pressure, 2.119 MN/m^2 (307.40 psia); percent hydrogen, 27.57; mixture ratio, 2.627.

spreads the data out along a line of -0.2 slope and that seemingly one line could be used for correlating all the stations. The slope would be far from -0.2 if one would attempt to correlate all stations with one line using Re_d.

Figure 10(a) is a plot of $St^* \; Pr^{*0.7}$ as a function of Re_x for all the data taken in reference 1 as well as the present data for all axial stations. A correlation of the form

$$St^* \; Pr^{*0.7} = C \; Re_x^{*-0.2}$$

correlates all the data for all stations for a $C = 0.0215$ with a 1σ variation = 0.0038. The 95-percent probability lines of reference 1 are also shown on this plot. In figure 10(b) the correlating equation and the 95-percent probability lines are replotted. The ◁ symbols on this plot are again the mean, the average highest C, and the average lowest C for four runs where data were taken at six circumferential locations. The spread is from 13.6 to -9.8 percent at the throat and from 17.6 to -14.1 percent in the chamber. The circumferential variation shown in this plot is for one running condition for the chamber and throat, respectively. The circumferential spread covers about half of the total spread of the correlation

$$St^* \; Pr^{*0.7} = 0.0215 \; Re_x^{*-0.2}$$

which covers all axial stations, all chamber pressures from 1.03 to approximately 6.895 MN/m^2 (150 to 1000 psia), and all mixture ratios from 2.57 to 8.1 (28 to 11 percent hydrogen). It also gives a designer some insight into how much of a safety margin would have to be allowed for in circumferential variations of heat transfer for a cooled thrust chamber design similar to this thrust chamber.

In order to further check the reliability of this correlation, the heated air data of reference 2 were used. These data are especially interesting because the cooled chamber length was varied. Figure 11 shows $St^* \; Pr^{*0.7}$ as a function of Re_x^* for chamber lengths of 0, 15.24, 30.48, and 45.72 centimeters (0, 6, 12, and 18 in.), where x is the distance from the chamber entrance. These runs were all heated air at 517.1 kN/m^2 (75 psia) and 883.3 K (1500° R). To increase the Reynolds number range, a run with a 45.72-centimeter (18-in.) chamber length is shown where the total pressure was increased to 1.72 MN/m^2 (250 psia). The equation $St^* \; Pr^{*0.7} = 0.0247 \; Re_x^{*-0.2}$ seems to correlate the combined data for all stations with a 1σ variation of 0.0047. Since the range of Reynolds number was small, the -0.2 slope customarily used for turbulent flow was retained. The 95-percent probability lines for these data are also shown on this plot. Figure 12 shows that using x instead of d for the Reynolds number makes the data follow a flat plate-like correlation. It also shows that acceleration effects do not reduce the

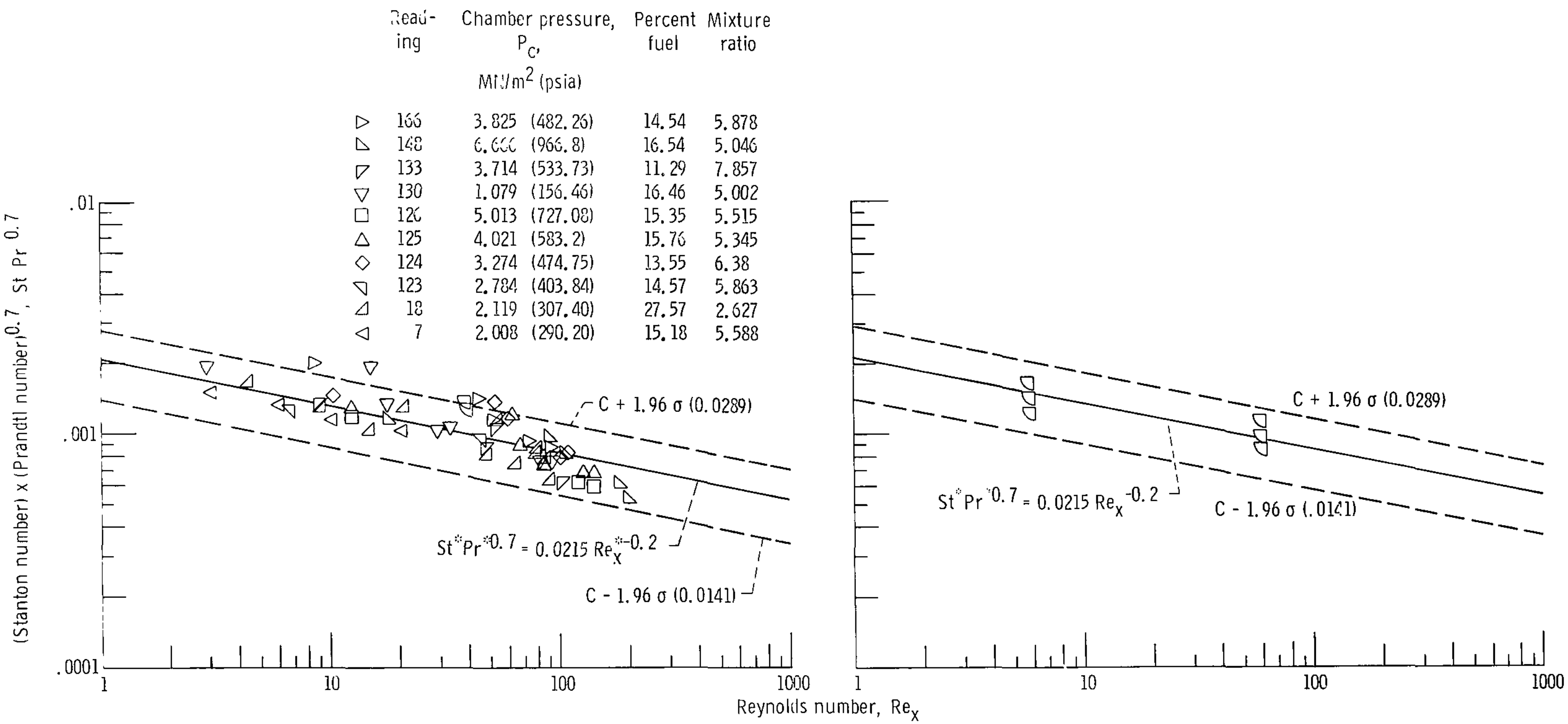

(a) For all stations, chamber pressures, and percent fuels.

(b) For circumferential variation. Runs 24, 27, 30, and 34; chamber pressure, 2.068 MN/m^2 (300 psia); percent fuel, 15; mixture ratio, 5.667.

Figure 10. - Product of Stanton number and (Prandtl number)$^{0.7}$ as function of Reynolds number.

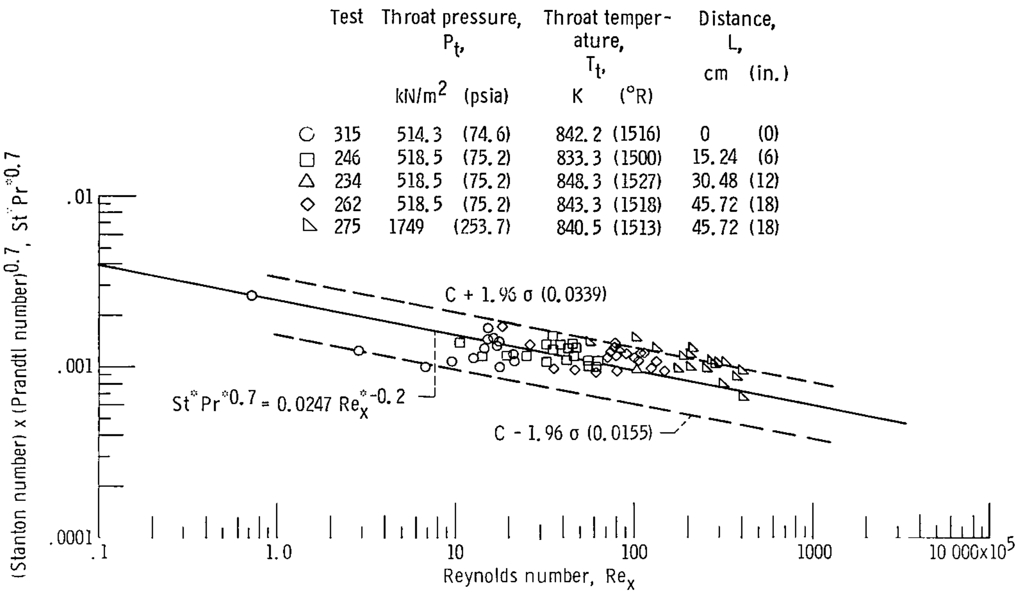

Figure 11. - Product of Stanton number and (Prandtl number)$^{0.7}$ as function of Reynolds number for JPL (ref. 2) data. Throat diameter, 4.58 centimeters (1.803 in.); contraction ratio, 7.75; expansion ratio, 2.68; one half convergence angle, 30 ; one half divergence angle, 15 .

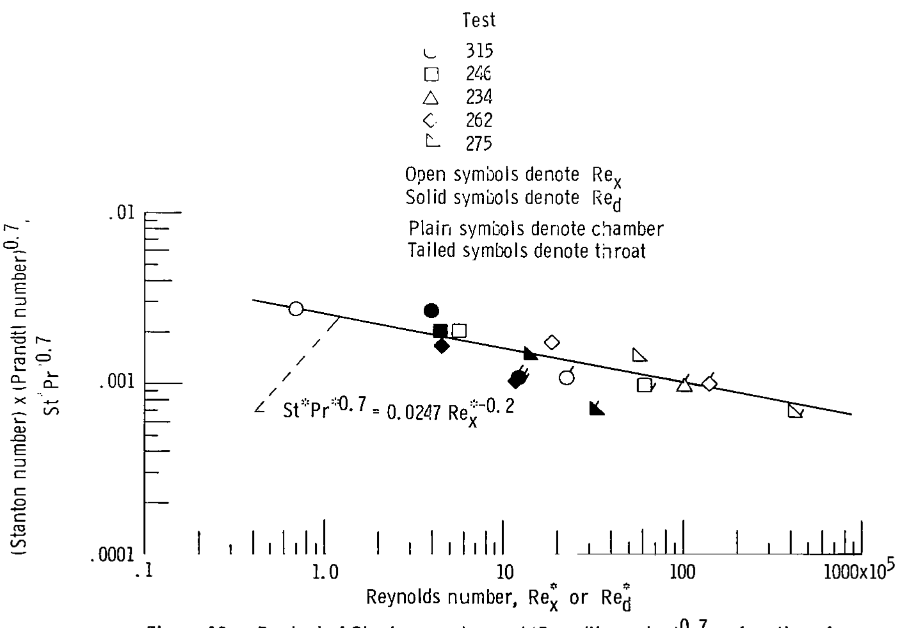

Figure 12. - Product of Stanton number and (Prandtl number)$^{0.7}$ as function of Reynolds number based on axial distance (Re_x^*) and on Reynolds number based on station diameter (Re_d^*) for JPL (ref. 2) data.

C to be used at the throat if an equation of the form $St^* \, Pr^{*0.7} = C \, Re_x^{* \, -0.2}$ is used for predicting the heat-transfer coefficient. The authors of reference 2 used the turbulent boundary-layer analysis of reference 8 where

$$\frac{h}{\rho_e u_e} C_p = K^* \frac{C_f^*}{2} \left(\frac{\varphi}{\theta}\right)^n$$

$$K^* = \left\{\sqrt{\frac{C_f^*}{2}}\left[5Pr + 5\ln(Pr + 1) - 14 + \sqrt{\frac{2}{C_f^*}}\right]\right\}^{-1}$$

The factor K^* is similar to the Prandtl number correction factor in the von Karman analogy. The coefficient C_f^* is analogous to the wall friction coefficient C_f but with the momentum thickness replaced by the energy thickness. When $n = 0$, the Stanton number depends only on the thermal characteristic φ. Therefore, the preceding equation becomes

$$\frac{h}{\rho_e u_e} C_p = K^* \frac{C_f^*}{2}$$

Using this equation, the authors of reference 2 predicted h for the 0-, 15.24-, and 45.72-centimeter (0-, 6-, and 18-in.) chamber lengths. Figure 13(a) is a plot of the ratio of h experimental to h predicted by the preceding equation for the various axial positions and the three different chamber lengths used in reference 2. A similar plot of the data of reference 2 is presented in figure 13(b) except that h experimental is divided by h predicted from a flat plate type of equation $St^* \, Pr^{*0.7} = 0.0247 \, Re_x^{* \, -0.2}$, where x was always measured from the beginning of the chamber. The same trends in the results are apparent in figures 13(a) and (b) with the simpler flat-plate-like correlation doing a slightly better job. This flat-plate type of correlation needs to be tried on more nozzles of different geometries, propellants, etc.

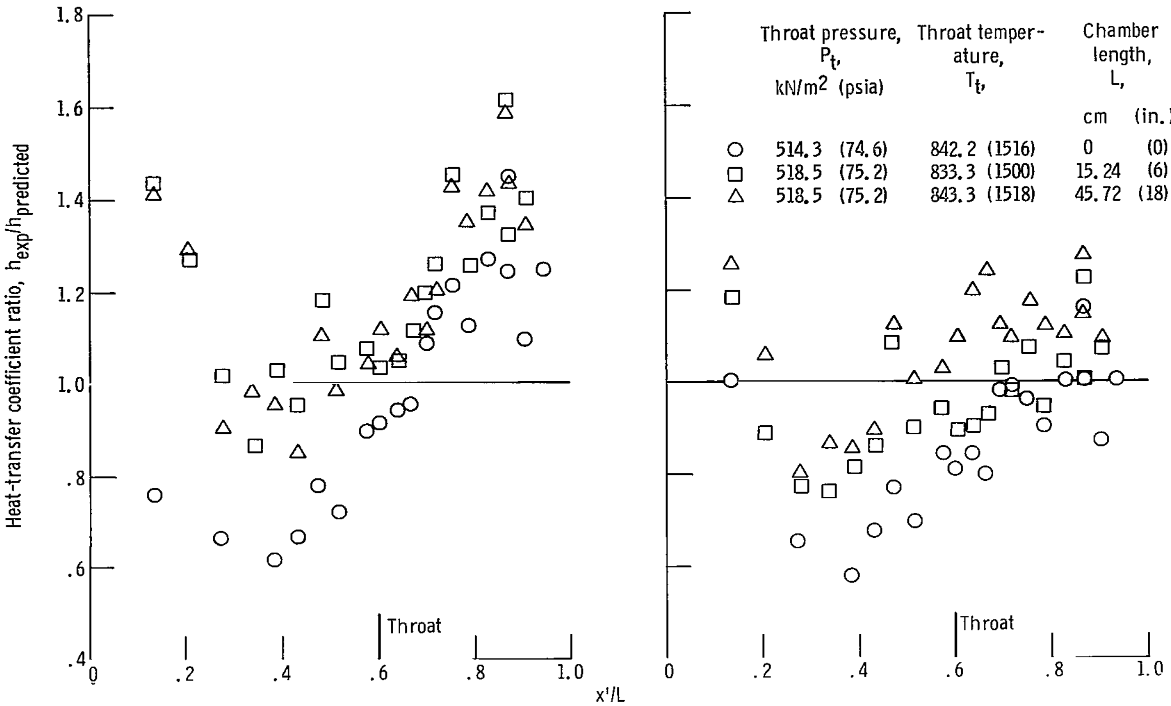

(a) Predicted using reference 8.

(b) Predicted using $St^{*}Pr^{*0.7} = 0.0247 Re_x^{*-0.2}$.

Figure 13. - Ratio of experimental heat transfer coefficients to those predicted for various inlet lengths.

CONCLUDING REMARKS

Although this particular thrust chamber and injector design had circumferential variations in q, these effects were investigated to the extent that it was determined that a valid axial correlation could be developed. In the light of the findings of this report, a word of warming must be given to a designer. He must design for his nozzle geometry and his injector. He must allow for circumferential effects. Because the methods for generating these data by experiment are now proven methods and are not too complicated, it seems feasible that one of the steps in the development of any new rocket system should be a heat-transfer experiment run early in the program perhaps in conjunction with injector stability tests. This is true only for designs that push the local cooling capabilities of the system; otherwise, large safety margins can be used in design and these tests bypassed. Simple correlations like $St^* Pr^{*0.7} = C Re_x^{*-0.2}$ or $St^* Pr^{*0.7} = C Re_d^{*-0.2}$ can be used. The Re_x type of correlation is recommended for the chamber region near the injector, especially for large diameter chambers with high contraction ratios.

SUMMARY OF RESULTS

An experimental investigation was conducted at NASA-Lewis to determine the axial and circumferential variations of heat-transfer coefficients in two rocket thrust chambers. Transient temperature measurements were made at 20 locations in one thrust chamber and at 18 locations in another thrust chamber. Six circumferential locations were used at the chamber and throat stations. The thrust chambers were operated over a range of mixture ratios from 2.57 to 5.67 (28 to 15 percent hydrogen) at a chamber pressure of 2.068 MN/m^2 (300 psia). Three injectors were used.

1. The data for all stations of this thrust chamber are correlated by the equation $St^* \, Pr^{*0.7} = 0.0215 \, Re_x^{*-0.2}$ with a 1σ variation of C equal to 0.0038, where St^*, Pr^*, and Re^* are reference Stanton, Prandtl, and Reynolds numbers, respectively, and C is a constant. When Re_d is used in this equation, the variation of data was twice that using Re_x, where d is the diameter and x is the axial distance from the injector.

2. The maximum circumferential variation of C in the chamber and throat are 38 and 27 percent, respectively.

3. In the throat region C was equal to 0.019, this is about 10 percent below the average value of C (0.0215 for all stations) when based on the equation $St^* \, Pr^{*0.7} = C \, Re_x^{*-0.2}$.

4. The Jet Propulsion Laboratory heated air data for a nozzle gave a $C = 0.0247$ with a 1σ variation of 0.0047 for all stations where Re_x was used.

Lewis Research Center,
National Aeronautics and Space Administration,
Cleveland, Ohio, March 22, 1971,
122-29.

APPENDIX - SYMBOLS

A	cross-sectional area
A^*	throat cross-sectional area
C	constant in equation $St^* \; Pr^{*0.7} = C \; Re^{*-0.2}$
C_f^*	coefficient analogous to skin-friction coefficient, with momentum thickness dependence replaced by energy thickness nozzle diameter
c	specific heat of material
D	nozzle diameter
H	enthalpy
H_{AW}	adiabatic wall enthalpy
h	heat-transfer coefficient
K^*	correction factor in the equation

$$K^* = \left\{ \sqrt{\frac{C_f^*}{2}} \left[5Pr + \ln(Pr + 1) - 14 + \sqrt{\frac{2}{C_f^*}} \right] \right\}^{-1}$$

k	thermal coefficient of conductivity of material
L	copper rod length
P	pressure
Pr	Prandtl number
q	heat flow rate per unit area
Re_d	Reynolds number based on diameter, $\rho^* V^d/\mu^*$
Re_x	Reynolds number based on axial length, $\rho^* V^x/\mu^*$
S	entropy
St	Stanton number
T	temperature
T_{AW}	adiabatic wall temperature, $f(H_{AW}, P_S)$
t	time

$\dot{w}$ total weight flow rate

x distance normal to heat surface

X axial distance from injector face

X^1 axial distance from nozzle inlet

θ momentum thickness

ρ material density

σ standard deviation

φ energy thickness

Subscripts:

c chamber or total

d based on diameter

e condition at free-stream edge of boundary layer

min minimum

w wall

s static

th throat

x based on distance from injector

0 zero burning time

Superscript:

* reference enthalpy condition

REFERENCES

1. Schacht, Ralph L.; Quentmeyer, Richard J.; and Jones, William L.: Experimental Investigation of Hot-Gas Side Heat-Transfer Rates for a Hydrogen-Oxygen Rocket. NASA TN D-2832, 1965.
2. Back, L. H.; Massier, P. F.; and Gier, H. L.: Convective Heat Transfer in a Convergent-Divergent Nozzle. Rep. TR 32-415, rev. 1, Jet Propulsion Lab., Calif. Inst. Tech. (NASA CR-57326), Feb. 15, 1965.
3. Carslaw, Horatio S.; and Jaeger, J. C.: Conduction of Heat in Solids. Second ed., Oxford Univ. Press, 1959, pp. 304-306.
4. Eckert, E. R.G.; and Drake, Robert M., Jr.: Heat and Mass Transfer. McGraw-Hill Book Co., Inc., 1950.
5. Zeleznik, Frank J.; and Gordon, Sanford: A General IBM 704 or 7090 Computer Program for Computation of Chemical Equilibrium Compositions, Rocket Performance, and Chapman-Jouguet Detonations. NASA TN D-1454, 1962.
6. Svehla, Roger A.: Thermodynamic and Transport Properties for the Hydrogen-Oxygen System. NASA SP-3011, 1964.
7. Von Glahn, Uwe H.: Correlation of Gas-Side Heat Transfer for Axisymmetric Rocket Engine Nozzles. NASA TM X-1748, 1969.
8. Elliott, David G.; Bartz, Donald R.; and Silver, Sidney: Calculation of Turbulent Boundary-Layer Growth and Heat Transfer in Axi-Symmetric Nozzles. Rep. TR-32-387, Jet Propulsion Lab., Calif. Inst. Tech., Feb. 15, 1963.

NASA-Langley, 1971 —— 33 E-5762

NATIONAL AERONAUTICS AND SPACE ADMINISTRATION
WASHINGTON, D.C. 20546

OFFICIAL BUSINESS
PENALTY FOR PRIVATE USE $300

FIRST CLASS MAIL

POSTAGE AND FEES PAID
NATIONAL AERONAUTICS AN
SPACE ADMINISTRATION

011 001 C1 U 33 710716 S00903DS
DEPT OF THE AIR FORCE
WEAPONS LABORATORY /WLOL/
ATTN: E LOU BOWMAN, CHIEF TECH LIBRARY
KIRTLAND AFB NM 87117

POSTMASTER: If Undeliverable (Section 158 Postal Manual) Do Not Retur

"The aeronautical and space activities of the United States shall be conducted so as to contribute . . . to the expansion of human knowledge of phenomena in the atmosphere and space. The Administration shall provide for the widest practicable and appropriate dissemination of information concerning its activities and the results thereof."

—NATIONAL AERONAUTICS AND SPACE ACT OF 1958

NASA SCIENTIFIC AND TECHNICAL PUBLICATIONS

TECHNICAL REPORTS: Scientific and technical information considered important, complete, and a lasting contribution to existing knowledge.

TECHNICAL NOTES: Information less broad in scope but nevertheless of importance as a contribution to existing knowledge.

TECHNICAL MEMORANDUMS: Information receiving limited distribution because of preliminary data, security classification, or other reasons.

CONTRACTOR REPORTS: Scientific and technical information generated under a NASA contract or grant and considered an important contribution to existing knowledge.

TECHNICAL TRANSLATIONS: Information published in a foreign language considered to merit NASA distribution in English.

SPECIAL PUBLICATIONS: Information derived from or of value to NASA activities. Publications include conference proceedings, monographs, data compilations, handbooks, sourcebooks, and special bibliographies.

TECHNOLOGY UTILIZATION PUBLICATIONS: Information on technology used by NASA that may be of particular interest in commercial and other non-aerospace applications. Publications include Tech Briefs, Technology Utilization Reports and Technology Surveys.

Details on the availability of these publications may be obtained from:

SCIENTIFIC AND TECHNICAL INFORMATION OFFICE

NATIONAL AERONAUTICS AND SPACE ADMINISTRATION

Washington, D.C. 20546